

Isolation and characterization of a novel uronic acid-containing acidic glycosphingolipid from the ascidian *Halocynthia roretzi*

Masahiro Ito,^{1,*} Yuki Matsumuro,^{*} So Yamada,^{*} Tomonori Kitamura,[†] Saki Itonori,[†] and Mutsumi Sugita[†]

Department of Bioscience and Bioinformatics,^{*} College of Information Science and Engineering, Ritsumeikan University, 1-1-1 Nojihigashi, Kusatsu, Shiga 525-8577, Japan; and Department of Chemistry,[†] Faculty of Liberal Arts and Education, Shiga University, 2-5-1 Hiratsu, Otsu, Shiga 520-0862, Japan

Abstract A novel uronic acid-containing glycosphingolipid (UGL-1) was isolated from the ascidian *Halocynthia roretzi*. UGL-1 was prepared from chloroform-methanol extracts and purified by the use of successive column chromatography on DEAE-Sephadex, Florisil, and Iatrobeads. Chemical structural analysis was performed using methylation analysis, gas chromatography, gas chromatography-mass spectrometry, matrix-assisted laser-desorption/ionization time-of-flight mass spectrometry, and ¹H-NMR spectra. The chemical structure of UGL-1 was determined to be a glucuronic acid-containing glycosphingolipid, Galβ1-4(Fucα1-3)GlcAβ1-1Cer. The ceramide component was composed of C16:0 and C18:0 acids and C₁₆, C₁₇, and C₁₈-phytosphingosines as major components.—Ito, M., Y. Matsumuro, S. Yamada, T. Kitamura, S. Itonori, and M. Sugita. Isolation and characterization of a novel uronic acid-containing acidic glycosphingolipid from the ascidian *Halocynthia roretzi*. *J. Lipid Res.* 2007. 48: 96–103.

Supplementary key words glucuronic acid • chemical structure • ceramide moiety • ¹H-nuclear magnetic resonance • matrix-assisted laser-desorption/ionization time-of-flight mass spectrometry

Glycosphingolipids have been characterized in a range of animal phyla, including arthropods, and have been shown to participate in important functions such as cellular development (1–6). Comparison of protostome and deuterostome glycolipids shows dramatic structural differences even between species with closely related glycolipid expression. In particular, the structures of acidic glycolipids are unique. The sialylated glycosphingolipids, called gangliosides, have been widely distributed within the Echinodermata and in deuterostomes. For example, although gangliosides have not been detected in protostomia, other

acidic glycosphingolipids containing uronic acid or inositol phosphate have been characterized (7–9).

Ascidians, which belong to the phylum Urochordata, are often referred to as protochordates because during the larval stage they possess chordate characteristics, most notably the tail contains a notochord and a dorsal hollow nerve cord. After a free-swimming stage, the simple tadpole-like larvae attach to a substrate and undergo metamorphosis that includes tail loss and rearrangement of the internal organs. Subsequently, in the adult form, the similarities to chordates are lost. In addition, ascidians are good model organisms for understanding vertebrates (and their development) because their cell lineage can be traced (10, 11) and a large number of genome-related data have been accumulated, including genome sequences, expressed sequence tag sequences, and gene expression patterns (12–15). However, very few studies have been directed to ascidian glycolipids, with the exception of some neutral glycolipids (16–18).

In this article, we describe the structural characterization of a novel acidic glycosphingolipid containing a uronic acid residue (UGL-1) from the ascidian *Halocynthia roretzi*. UGL-1 exhibits unique structural features, such as Galβ1-4(Fucα1-3)GlcAβ1-1Cer. The chemical structure of UGL-1, which has a uronic acid with a fucosyl residue bond at the reducing end, is the first example to our knowledge.

MATERIALS AND METHODS

Isolation and purification of acidic glycolipids

Specimens of *H. roretzi* were obtained from Hiroyo Fisheries, Ltd., at Miyagi in Japan, and the cellulose crust was removed,

Manuscript received 10 July 2006 and in revised form 22 September 2006 and in re-revised form 28 September 2006 and in re-re-revised form 3 October 2006.

Published, JLR Papers in Press, October 5, 2006.
DOI 10.1194/jlr.M600296-JLR200

Abbreviations: MALDI-TOF MS, matrix-assisted laser-desorption/ionization time-of-flight mass spectrometry; PSD, postsorce decay; UGL, uronic acid-containing glycosphingolipid.

[†]To whom correspondence should be addressed.

e-mail: maito@is.ritsumei.ac.jp

Copyright © 2007 by the American Society for Biochemistry and Molecular Biology, Inc.

suspended in acetone, and dried naturally. The dry *H. roretzi* (830 g) were homogenized using a mixer and extracted twice with chloroform-methanol (2:1, v/v) for 2 h and once with chloroform-methanol (1:1, v/v) overnight at room temperature. The extracts were combined and concentrated by a rotary evaporator at 40°C. The crude lipid fraction was subjected to mild alkaline hydrolysis to eliminate glycerolipids. The resulting precipitate of alkali-stable product was applied to a DEAE-Sephadex A-25 (Amersham Pharmacia Biotech) column (column size, 3.4 cm × 22 cm; acetate form). The acidic glycosphingolipid fraction was eluted with 5 volumes of 0.05 M ammonium acetate in methanol, altered to an acetyl derivative by the addition of pyridine/anhydride at 20°C for 18 h, and then applied to a Florisil (magnesium silicate; Nacalai Tesque) column (column size, 1.8 cm × 100 cm). The acidic glycosphingolipid fraction was eluted with 3 volumes of 1,2-dichloroethane-methanol (3:1, v/v), deacetylated, and neutralized by the addition of an appropriate amount of HCl.

The acidic glycosphingolipid fraction was rechromatographed on an Iatrobeds (silica gel 6RS-8060; Mitsubishi Kagaku Iatron, Inc.) column (column size, 1.2 cm × 120 cm) with a two-step linear gradient in chloroform-methanol-water (80:20:1; 650 ml) to chloroform-methanol-water (50:50:5; 730 ml). The fractions were collected in test tubes, checked by TLC, and assessed directly by matrix-assisted laser-desorption/ionization time-of-flight mass spectrometry (MALDI-TOF MS).

TLC

For TLC separation, TLC-silica gel 60 plates (E. Merck) were developed with chloroform-methanol-water (60:40:10, v/v/v) as the running solvent. The glycosphingolipids were visualized by spraying with orcinol/H₂SO₄ reagent for sugars, 5% H₂SO₄/ethanol reagent for organic substances, and ninhydrin reagent for free amino groups, followed by heating. Detection was performed with Dittmer-Lester reagent for phosphorus, azure-A reagent for sulfate, and resorcinol reagent for sialic acid.

MALDI-TOF MS

MALDI-TOF MS analysis of the purified UGL-1 was performed using an Applied Biosystems/Voyager-DE STRTM Biospectrometer with a nitrogen laser (337 nm) and an acceleration voltage of 20 kV, operating in the reflector positive and negative ion modes. Samples were analyzed in delayed extraction mode, postsources decay (PSD), using an acceleration voltage of 20 kV, a pulse delay time of 100 ns, and a grid voltage of 75%. The resolution of timed ion selector for the precursor ion was set at 80. The matrices used were 2,5-dihydroxybenzoic acid (Wako Pure Chemical Industries, Ltd.) and coumarin 120 (7-amino-4-methyl-coumarin; Sigma Chemical Co.). External mass calibration of MALDI-TOF MS was provided by the [M-H]⁻ ion of a glucuronic acid-containing ceramide octasaccharide (at *m/z* 1,940.0) prepared from the fresh water bivalve *Hyriopsis schlegelii* (19) in the reflector negative ion mode, the [M+Na]⁺ ions of ceramide trisaccharide (at *m/z* 1,064.7) and pentasaccharide (at *m/z* 1,471.1) prepared from the green-bottle fly *Lucilia caesar* (20, 21) in the reflector positive ion mode, and the [M+Na]⁺ ion of angiotensin I (at *m/z* 1,296.7) from Sigma Chemical Co. in the PSD positive ion mode.

Sugar and ceramide analysis

UGL-1 was hydrolyzed by microwave exposure with 0.1 M NaOH/methanol for 2 min followed by 1 M HCl/methanol for 45 s (22). The fatty acid methyl esters of unnecessary reaction products, such as *O*-methyl ethers, were removed by three extractions in 0.5 ml of *n*-hexane and then analyzed using the Shimadzu GC-18A gas chromatograph with the Shimadzu

HiCap-DBP5 (0.22 mm × 25 m) programmed at 2°C/min from 170°C to 230°C. The other products were neutralized with silver carbonate and then *N*-acetylated with pyridine-acetic anhydride in methanol at room temperature for 30 min. The *N*-acetylated products were trimethylsilylated with pyridine-hexamethyldisilazane-trimethylchlorosilane (9:3:1, v/v/v) at 60°C for 30 min (23). An aliquot of the residues was analyzed by gas chromatography as described above with the capillary column programmed at 2°C/min from 140°C to 230°C. Sphingoids prepared from glycolipids by methanolysis with 1 M aqueous methanolic HCl at 70°C for 18 h were converted into *O*-trimethylsilyl derivatives and then analyzed by GC on the same capillary column using a temperature program of 2°C/min from 210°C to 230°C.

Linkage analysis

For the determination of sugar linkages, 200 μg of each purified glycolipid was partially methylated with NaOH and methyl iodide in DMSO for 2 min (24), acetylated and hydrolyzed with 300 μl of HCl/water/acetic acid (0.5:1.5:8, v/v/v) in a microwave oven for 20 s, and then reduced with NaBH₄ and acetylated with acetic anhydride-pyridine (1:1, v/v) at 100°C for 12 min. The obtained reaction products were analyzed by GC and GC-MS (GCMS-QP; Shimadzu) on the same capillary column programmed at 4°C/min from 140°C to 230°C for GC and from 80°C (2 min) to 180°C (20°C/min) to 240°C (4°C/min) for GC-MS.

Reduction of the carbonic acid group on uronic acid

For the reduction of uronic acid, 100 μg of UGL-1 was treated with 1-ethyl-3-(3-dimethylaminopropyl) carbodiimide (20 mg/ml) in water and 0.01 M HCl (pH 4.7–5.0) for 2 h, which was then shifted to pH ~ 8 with ammonium hydroxide, and then stirred with 10 mg of sodium borohydride and several drops of butanol at 55°C for 18 h. The reaction was stopped with several drops of acetic acid, and then the obtained reduced sample was dialyzed and concentrated.

Partial acid hydrolysis

To remove a fucose residue, partial acid hydrolysis was carried out by treatment of the reduced sample (200 μg) with 0.1 M HCl at 100°C for 30 min. The degradation products were isolated by Iatrobeds column chromatography. The obtained reaction products were analyzed by GC and GC-MS under the same conditions described above.

¹H-NMR spectroscopy

The purified glycolipid was dissolved in 0.60 ml of [²H₆]DMSO + 0.05% (v/v) tetramethylsilane (Wako Pure Chemical Industries, Ltd.) containing 2% ²H₂O (Nacalai Tesque, Inc.), and chemical shift was referenced to trimethylsilyl (δ_H 0.00 ppm) as the internal standard. ¹H-NMR spectra of purified UGL-1 (1.0 mg) was recorded on a 400 MHz spectrometer (JEOL, Ltd.; A-400) in the NMR tube (~5 mm; Kusano Science Co.) at an operating temperature of 60°C. The obtained NMR spectra data were analyzed with 1D, 2D Application software (<http://nakamura-2.ees.hokudai.ac.jp/nmr/nmr.html>).

RESULTS

Isolation and TLC analysis of acidic glycolipids from *H. roretzi*

Total acidic glycosphingolipid of the ascidian *H. roretzi* as obtained by DEAE-Sephadex A-25 and Florisil column

chromatography comprised a mixture of several major compounds (Fig. 1). The one species was separated by Iatrobeds column chromatography, yielding a uronic acid-containing glycosphingolipid, called UGL-1. TLC analysis of UGL-1 showed positive reactions with orcinol/ H_2SO_4 reagent (Fig. 1) and negative reactions with Dittmer-Lester, ninhydrin, azure-A, and resorcinol reagents (data not shown).

Ceramide analysis

Characterization of the ceramide moiety was performed by GC and GC-MS analyses. Glycolipids were subjected to the same procedures of fatty acid determination (see Materials and Methods). However, for sphingoid analysis, methanolysis of UGL-1 afforded only small amounts of sphingoids, most likely owing to the attachment of glucuronic acid, which may interfere with acidic cleavage. When UGL-1 was reduced by sodium borohydride before methanolysis, three long-chain bases were detected and analyzed by GC and GC-MS, as with acetylated derivatives.

The main fatty acids of UGL-1 were C16:0 and C18:0; the minor fatty acid component h24:0 was also present. The sphingoids were composed entirely of C₁₆, C₁₇, and C₁₈-phytosphingosines in UGL-1 (Table 1).

Sugar analysis of UGL-1

To determine the sugar components of UGL-1, compositional analysis of UGL-1 was first carried out by the methanolysis method using GC. The composition of UGL-1 was determined to be fucose-galactose in a ratio of 1:1 (Table 2). Although UGL-1 was fractionated into the acidic fraction by ion-exchange column chromatography, UGL-1 showed negative reactions with Dittmer-Lester, azure-A, and resorcinol reagents on TLC. From the results of sugar, TLC (shown above), and PSD fragments from

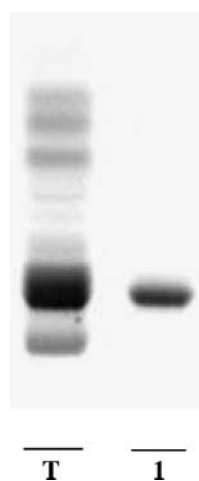


Fig. 1. TLC of purified uronic acid-containing glycosphingolipid-1 (UGL-1) from *H. roretzi*. TLC was performed using chloroform-methanol-water (60:40:10, v/v/v) and visualized by orcinol/ H_2SO_4 staining. Lane T, whole acidic glycolipids from *H. roretzi*; lane 1, UGL-1 obtained from *H. roretzi*.

TABLE 1. Ceramide moiety of UGL-1

Fatty Acid	Percent	Sphingoid	Percent
14:0	6.9	t16:0	26.0
16:0	25.6	t17:0	12.0
18:0	15.7	t18:0	62.0
18:1	10.3		
20:0	9.6		
22:0	4.6		
24:0	3.4		
h18:0	3.5		
h20:0	4.3		
h22:0	6.7		
h24:0	9.4		

UGL-1, uronic acid-containing glycosphingolipid-1. Ceramide moieties of deoxidized glycolipid monosaccharides were analyzed by GC and GC-MS (see Materials and Methods).

MALDI-TOF MS analysis (shown below), the acidic carbohydrate of UGL-1 was estimated to contain a uronic acid residue.

After UGL-1 was reduced with sodium borohydride (see Materials and Methods), sugar compositional analysis was carried out by the methanolysis method using GC. When sugar composition compared reduced UGL-1 with intact UGL-1, the reduced UGL-1 showed an increased glucose residue. The sugar composition of reduced UGL-1 was found to be fucose-galactose-glucose in a ratio of 1:1:1 (Table 2). Therefore, the sugar composition of UGL-1 was identified as fucose-galactose-glucuronic acid in a ratio of 1:1:1.

MALDI-TOF MS analysis

UGL-1 was characterized by several molecular masses in reflector negative and positive ion modes using MALDI-TOF MS (Fig. 2, Table 3). The two highest peaks in each mode were found at m/z 1,152.7 and 1,154.7 in negative ion mode (Fig. 2A) and at m/z 1,176.5 and 1,178.6 in positive ion mode (Fig. 2B). The differences in m/z values between positive and negative ion modes correspond to molecular masses of 23.8 and 23.9 Da, which are attributable to the molecular mass of Na plus H.

The putative structure of the purified UGL-1 was confirmed by MALDI-TOF MS analysis in the negative ion mode (Fig. 2A). Peaks at m/z 1,126.6, 1,140.7, 1,152.7, 1,154.7, and 1,168.7 were detected as major peaks, in addition to those at m/z 1,112.6, 1,124.6, 1,138.6, 1,166.7, 1,180.7, and 1,182.7. Small peaks at m/z 1,108.6, 1,110.6, 1,122.6, 1,136.6, 1,146.6, 1,150.6, 1,160.6, and 1,174.6 were also detected from UGL-1. Based on the difference of cer-

TABLE 2. Sugar components of UGL-1

UGL	Saccharide		
	Galactose	Fucose	Glucose
UGL-1	1.00	0.74	—
Reduced UGL-1	1.00	0.76	0.89

Values shown are molar ratios. Purified and reduced glycolipid monosaccharides were prepared by the methanolysis method and analyzed by GC (see Materials and Methods).

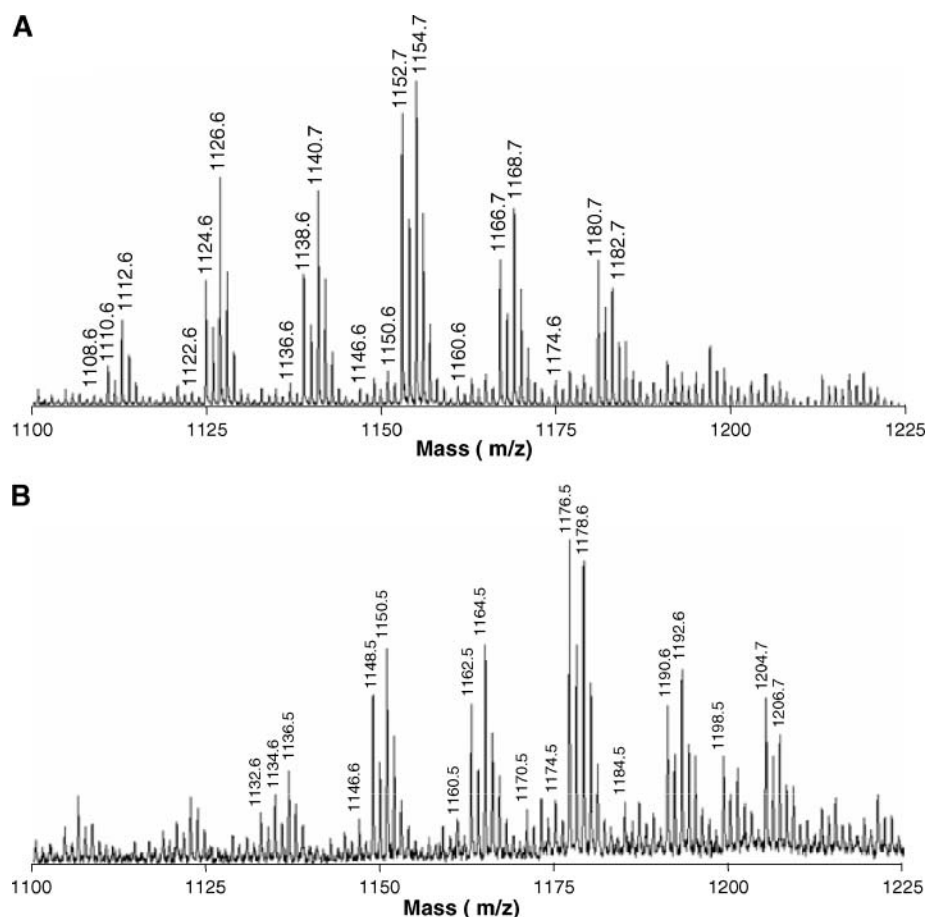


Fig. 2. Matrix-assisted laser-desorption/ionization time-of-flight mass spectrometry (MALDI-TOF MS) analyses of *H. roretzi* UGL-1. UGL-1 obtained after Iatrobeds column separation was monitored as $[M-H]^-$, $[M+Na-2H]^-$, and $[M+Na-2H]^-$ ions in the reflector negative ion mode (A) and as $[M+Na]^+$, $[M-H+2Na]^+$, and $[M-2H+3Na]^+$ ions in the reflector positive ion mode (B) by MALDI-TOF MS with the coumarin 120 matrix. These results are summarized in Table 3.

amide composition in UGL-1, these major peaks formed six islands or three groups. For example, in the case of peaks at m/z 1,112.6, 1,126.6, 1,140.7, 1,154.7, 1,168.7, and 1,182.7, the difference of each molecular mass is ~ 14 Da. This value is similar to the molecular mass of CH_2 . Furthermore, it was similar in the case of peaks at m/z 1,110.6, 1,124.6, 1,138.6, 1,152.7, 1,166.7, and 1,180.7.

Based on consideration of molecular weight comprising the sugar component and the ceramide moiety, peaks detected as major peaks were determined with $[M-H]^-$ and $[M+2Na-3H]^-$ ions. On the other hand, small peaks were determined with $[M+Na-2H]^-$ and $[M-H]^-$ ions. These ionizations were identified by MALDI-TOF MS analysis using a saturated solution of 2,3-dihydroxybenzoic acid in 40 mM aqueous LiCl as the matrix (25). The putative structure of the purified UGL-1 was also identified by MALDI-TOF MS analysis in the positive ion mode (Fig. 2B). The summary of MALDI-TOF MS analysis is shown in Table 3.

The MALDI-TOF MS analysis of PSD fragments was carried out for several main peaks of UGL-1. The PSD fragment analysis of precursor mass at m/z 1,176.5 is shown in Fig. 3. In the case of UGL-1, from the difference of

ceramide composition, the former was characterized by $[M+Na]^+$ molecular masses of m/z 1,163.3, 1,177.8, and 1,192.3 (Fig. 3). Fragment ions of $[ceramide+Na]^+$ at m/z 677.5, 692.6, and 707.7, which were derived from the ceramide moiety, showed the same heterogeneous pattern. The fragment ion at m/z 507.0 of $[Hex(dHex)HexA-H_2O+Na]^+$, which was derived from the sugar component, was included with UGL-1. These data also showed that UGL-1 had trisaccharide carbohydrate moieties with different ceramide moieties.

Linkage analysis

To determine sugar linkages, UGL-1 was prepared as partially methylated alditol acetates for analysis of substitution positions by GC and GC-MS (Table 4, Fig. 4). Methylation analysis of UGL-1 showed the presence of 1,5-di-*O*-acetyl-2,3,4-tri-*O*-methylfucitol (1Fuc) and 1,5-di-*O*-acetyl-2,3,4,6-tetra-*O*-methylgalactitol (1Gal) (Fig. 4A). Here, as with methanolysis analysis, the glucuronic acid residue was not detected by partial methylated alditol acetate analysis.

UGL-1 was reduced by sodium borohydride and prepared as partially methylated alditol acetates for analysis of

TABLE 3. Summary of matrix-assisted laser-desorption/ionization time-of-flight mass spectrometry analysis of UGL-1

Negative Ion			Positive Ion			Composition
Measured	Calculated	Ionization	Measured	Calculated	Ionization	Fatty Acid-Sphingoid
1,108.6	1,108.6	$[M+2Na-3H]^-$	1,132.6	1,132.6	$[M-2H+3Na]^+$	C18:1-t18:0
	1,108.7	$[M-H]^-$		1,132.7	$[M+Na]^+$	C22:0-t17:0
1,110.6	1,110.7	$[M-H]^-$	1,134.6	1,134.7	$[M+Na]^+$	h22:0-t16:0
		$[M+2Na-3H]^-$			$[M-2H+3Na]^+$	h20:0-t18:0
						C20:0-t16:0
1,112.6	1,112.6	$[M+2Na-3H]^-$	1,136.5	1,136.6	$[M-2H+3Na]^+$	C18:0-t18:0
1,122.6	1,122.8	$[M-H]^-$	1,146.6	1,146.7	$[M+Na]^+$	h18:0-t17:0
						C24:0-t16:0
						C22:0-t18:0
1,124.6	1,124.7	$[M-H]^-$	1,148.5	1,148.7	$[M+Na]^+$	h22:0-t17:0
		$[M+2Na-3H]^-$			$[M-2H+3Na]^+$	C20:0-t17:0
1,126.6	1,126.6	$[M+2Na-3H]^-$	1,150.5	1,150.6	$[M-2H+3Na]^+$	h20:0-t16:0
						h18:0-t18:0
1,136.6	1,136.7	$[M-H]^-$	1,160.5	1,160.8	$[M+Na]^+$	C24:0-t17:0
1,138.6	1,138.7	$[M-H]^-$	1,162.5	1,162.7	$[M+Na]^+$	h24:0-t16:0
						h22:0-t18:0
		$[M+2Na-3H]^-$			$[M-2H+3Na]^+$	C22:0-t16:0
						C20:0-t18:0
1,140.7	1,140.7	$[M+2Na-3H]^-$	1,164.5	1,164.7	$[M-2H+3Na]^+$	h20:0-t17:0
1,146.6	1,146.7	$[M+Na-2H]^-$	1,170.5	1,170.7	$[M-H+2Na]^+$	h22:0-t17:0
1,150.6	1,150.8	$[M-H]^-$	1,174.5	1,174.8	$[M+Na]^+$	C24:0-t18:0
1,152.7	1,152.7	$[M+2Na-3H]^-$	1,176.5	1,176.7	$[M-2H+3Na]^+$	C22:0-t17:0
	1,152.8	$[M-H]^-$		1,176.8	$[M+Na]^+$	h24:0-t17:0
1,154.7	1,154.7	$[M+2Na-3H]^-$	1,178.6	1,178.7	$[M-2H+3Na]^+$	h22:0-t16:0
						h20:0-t18:0
1,160.6	1,160.7	$[M+Na-2H]^-$	1,184.5	1,184.7	$[M-H+2Na]^+$	h24:0-t16:0
						h22:0-t18:0
1,166.7	1,166.7	$[M+2Na-3H]^-$	1,190.6	1,190.7	$[M-2H+3Na]^+$	C24:0-t16:0
						C22:0-t18:0
	1,166.8	$[M-H]^-$		1,190.8	$[M+Na]^+$	h24:0-t18:0
1,168.7	1,168.7	$[M+2Na-3H]^-$	1,192.6	1,192.7	$[M-2H+3Na]^+$	h22:0-t17:0
1,174.6	1,174.7	$[M+Na-2H]^-$	1,198.5	1,198.7	$[M-H+2Na]^+$	h24:0-t17:0
1,180.7	1,180.7	$[M+2Na-3H]^-$	1,204.7	1,204.7	$[M-2H+3Na]^+$	C24:0-t17:0
1,182.7	1,182.7	$[M+2Na-3H]^-$	1,206.7	1,206.7	$[M-2H+3Na]^+$	h24:0-t16:0
						h22:0-t18:0

substitution positions by GC and GC-MS (Fig. 4B). As a result, 1,3,4,5-tetra-*O*-acetyl-2,6-di-*O*-methyl-*N*-acetylglucitol (1,3,4Glc) was detected in reduced UGL-1. Furthermore, to determine the linkage position of the two

reducing terminal sugar residues (galactose and fucose) to glucuronic acid, methylation analysis was performed with reduced UGL-1 after defucose processing by partial acid hydrolysis. Methylation analysis of reduced UGL-1 showed

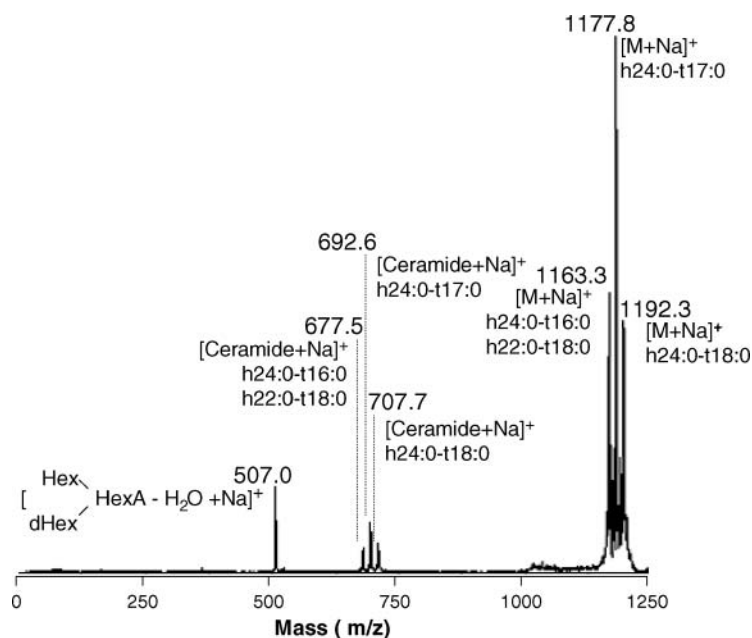


Fig. 3. Postsource decay fragments from MALDI-TOF MS analysis of *H. roretzi* UGL-1. UGL-1 was monitored with 2,5-dihydroxybenzoic acid in the postsource decay positive ion mode. The precursor mass was set at m/z 1,176.5. The resolution of timed ion selector for the precursor ion was set at 80, which would allow a mass window of ~ 30 Da.

TABLE 4. Methylation analysis of UGL-1

UGL	Saccharide		
	Galactose	Fucose	Glucose
UGL-1	1	1	—
Deoxidized UGL-1	1	1	1,3,4
Defucosylated and reduced UGL-1	1	—	1,4

Values shown are substitution positions. Native and reduced and defucosylated glycolipid monosaccharides were prepared as partially methylated alditol acetates and analyzed by GC-MS (see Materials and Methods).

the presence of 1,5-di-*O*-acetyl-2,3,4,6-tetra-*O*-methylgalactitol (1Gal) and 1,4,5-tri-*O*-acetyl-2,3,6-tri-*O*-methylglucitol (1,4Glc) (Fig. 4C).

Anomeric configuration analysis

To determine the anomeric configuration of the sugar residues, UGL-1 was subjected to ^1H -NMR spectroscopy (Fig. 5). In the anomeric region of the spectrum for UGL-1, the following anomeric proton resonances were observed: at 4.21 ppm ($J_{1,2}$ 7.5 Hz), demonstrating β -glucuronic acid residue; at 4.30 ppm ($J_{1,2}$ 6.4 Hz), demonstrating β -galactose residue; and at 5.15 ppm ($J_{1,2}$ 2.1 Hz), demonstrating α -fucose residue. Furthermore, the H5 proton resonance of the α -fucose residue was observed at 4.55 ppm ($J_{1,2}$ 6.3 Hz).

These results suggested that the chemical structure of UGL-1 was Gal β 1-4(Fuc α 1-3)Glc α 1-Cer.

DISCUSSION

From the ascidian *H. roretzi*, we propose the chemical structure of the novel UGL-1, characterized as Gal β 1-4(Fuc α 1-3)Glc α 1-Cer (Fig. 6).

Glycosphingolipids are widely found as cellular constituents of marine and terrestrial animals, and they are believed to possess several interesting biological activities, including modulation of growth and regulation of differentiation. It is also commonly acknowledged that this bioactivity depends essentially on the nature of the functionalized structure of the molecule, including the carbohydrate moiety. In invertebrates, glucuronic acid-containing glycosphingolipids have been characterized from flies, *Lucilia caesar* (7) and *Drosophila melanogaster* (26), and in arthropods located at the top of the protostomia. From the Echinodermata, located downstream of the Urochordata, invertebrate deuterostomes, gangliosides, and sulfatide have been characterized (27–31), and characterization of glucuronic acid-containing glycosphingolipids has not yet been reported. On the other hand, in vertebrates, glucuronic acid-containing glycosphingolipids and sulfated glucuronyl glycosphingolipids have been characterized from the HNK-1 epitope in humans and mice (32, 33). HNK-1 has not yet been identified from ascidians, although recently it was identified from the lancelet in the Urochordata, similar to ascidians, and from the sea urchin in the Echinodermata (34). It is very interesting in terms of evolution and function that the novel structures of glucuronic acid-containing glycosphingolipids were characterized in invertebrate ascidians, which is nearest to the vertebrates.

Acidic glycosphingolipids, gangliosides, and sulfated glucuronic acid-containing glycosphingolipids are located in the outer leaflet of the plasma membrane, being expressed at the surface of various cell types and widely distributed in vertebrates, especially in the nervous system of mammals (35, 36). As ascidians are classified as invertebrates, which are close to vertebrates, we think that the analysis and comparison of the cellular localization of UGL-1 represent a shortcut for understanding the function of glycosphingolipids.

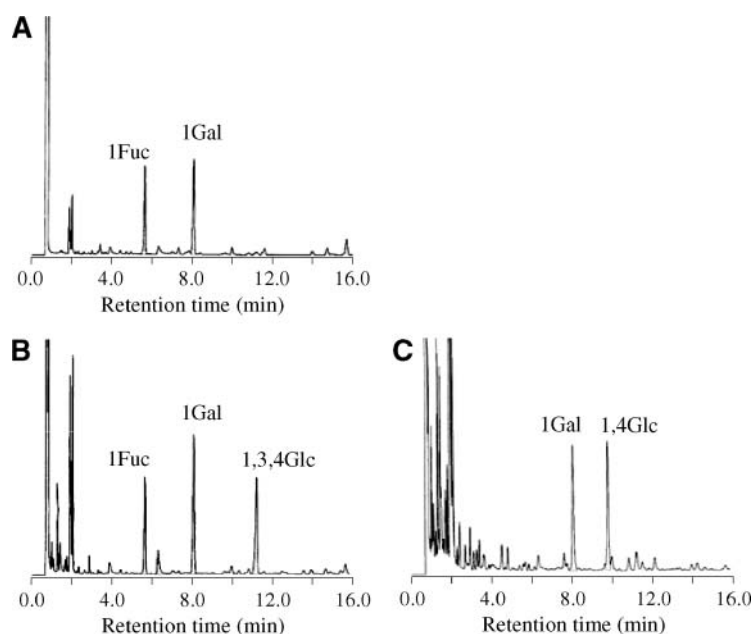


Fig. 4. Linkage analysis of *H. roretzi* UGL-1. Intact UGL-1 (A), reduced UGL-1 (B), and reduced and defucosylated UGL-1 (C) were monitored by GC. 1Fuc, 1,5-di-*O*-acetyl-2,3,4-tri-*O*-methylfucitol; 1Gal, 1,5-di-*O*-acetyl-2,3,4,6-tetra-*O*-methylgalactitol; 1,3,4Glc, 1,3,4,5-tetra-*O*-acetyl-2,6-di-*O*-methyl-*N*-acetylglucitol; 1,4Glc, 1,4,5-tri-*O*-acetyl-2,3,6-tri-*O*-methylglucitol.

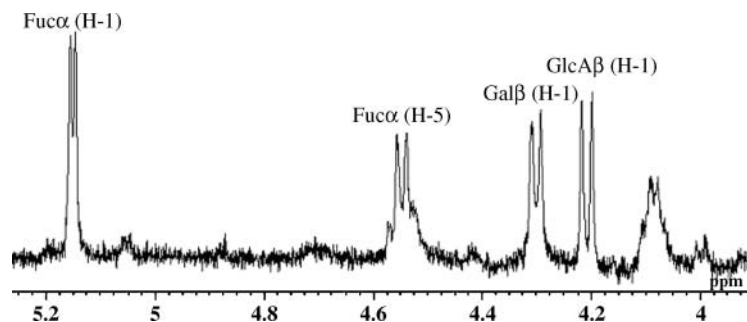



Fig. 5. ^1H -NMR spectrum of *H. roretzi* UGL-1. Anomeric protein regions of UGL-1 are indicated.

The presence of a neutral glycosphingolipid (sulcaceramide) has been reported in the ascidian *Microcosmus sulcata* (18). The sulcaceramide is a structural analog of UGL-1 that replaced glucuronic acid with glucose, $\text{Gal}\beta 1\text{-4}$ ($\text{Fuc}\alpha 1\text{-3}$) $\text{Glc}\beta 1\text{-1Cer}$. The biosynthetic pathways of ascidian glycosphingolipids are still little known. The structural characterization of the ascidian glycosphingolipids leads us to propose several biosynthetic pathways involving the addition of glucose or glucuronic acid to ceramide or the conversion of the 6-position group on glucose and glucuronic acid. The significance of such a unique acid glycolipid on the cell surface remains to be elucidated. However, glucuronic acid-containing glycosphingolipids have been reported from the bacterium *Sphingomonas paucimobilis* (37, 38). Glycosphingolipids in *S. paucimobilis* have been characterized as $\text{GalA}\alpha\text{-Cer}$ and $\text{Man}\alpha 1\text{-2Gal}\alpha 1\text{-5GlcN}\alpha 1\text{-4GlcA}\alpha 1\text{-1Cer}$ and contained no lipopolysaccharide-like molecules. These findings on the cellular lipids of *S. paucimobilis* prompted the investigation of the cell surface structure of this Gram-negative bacterium and the physiological roles of the glycosphingolipids (39).

Thus, the finding in *H. roretzi* of a novel acidic glycosphingolipid, characterized by a unique sugar portion, suggests that glycosphingolipids also play an essential biological role in ascidians. In the near future, we expect an increasing amount of activity in this field on account of the recent improvements in spectroscopic and isolation techniques; it is now possible to perform conclusive structural determination studies on very small quantities

of pure compounds, like those usually obtained from the extracts of most ascidians. 

This work was supported in part by a Grant-in-Aid for Young Scientists B and a High-Tech Research Center Project for Private Universities matching fund subsidy from the Ministry of Education, Culture, Sports, Science, and Technology of Japan to M.I.

REFERENCES

- Blackburn, C. C., P. Swank-Hill, and R. L. Schnaar. 1986. Gangliosides support neural retina cell adhesion. *J. Biol. Chem.* **261**: 2873–2881.
- Hakomori, S.-i., and Y. Igarashi. 1993. Gangliosides and glycosphingolipids as modulators of cell growth, adhesion and transmembrane signaling. *Adv. Lipid Res.* **25**: 147–162.
- Hakomori, S.-i., and Y. Igarashi. 1995. Functional role of glycosphingolipids in cell recognition and signaling. *J. Biochem. (Tokyo)*. **118**: 1091–1103.
- Rietveld, A., S. Neutz, K. Simons, and S. Eaton. 1999. Association of sterol- and glycosylphosphatidylinositol-linked proteins with *Drosophila* raft lipid microdomains. *J. Biol. Chem.* **274**: 12049–12054.
- Inokuchi, J., K. Kabayama, S. Uemura, and Y. Igarashi. 2004. Glycosphingolipids govern gene expression. *Glycoconj. J.* **20**: 169–178.
- Aixinjueluo, W., K. Furukawa, Q. Zhang, K. Hamanura, N. Tokuda, S. Yohsida, R. Ueda, and K. Furukawa. 2005. Mechanisms for the apoptosis of small cell lung cancer cells induced by anti-GD2 monoclonal antibodies: role of anoikis. *J. Biol. Chem.* **280**: 29828–29836.
- Sugita, M., S. Itonori, F. Inagaki, and T. Hori. 1989. Characterization of two glucuronic acid-containing glycosphingolipids in larvae of the green-bottle fly, *Lucilia caesar*. *J. Biol. Chem.* **264**: 15028–15033.
- Sugita, M., T. Mizunoma, K. Aoki, J. T. Dulaney, F. Inagaki, M. Suzuki, A. Suzuki, S. Ichikawa, K. Kushida, S. Ohta, et al. 1996. Structural characterization of a novel glycoinositolphospholipid from the parasitic nematode, *Ascaris suum*. *Biochim. Biophys. Acta*. **1302**: 185–192.
- Itonori, S., and M. Sugita. 2005. Diversity of oligosaccharide structures of glycosphingolipids in invertebrates. *Trends Glycosci. Glycotech.* **17**: 15–25.
- Nishida, H., and N. Satoh. 1985. Cell lineage analysis in ascidian embryos by intracellular injection of a tracer enzyme. II. The 16- and 32-cell stages. *Dev. Biol.* **110**: 440–454.
- Nishida, H. 1987. Cell lineage analysis in ascidian embryos by intercellular injection of a tracer enzyme. III. Up to the tissue restricted stage. *Dev. Biol.* **121**: 526–541.
- Dehal, P., Y. Satou, R. K. Campbell, J. Chapman, B. Degnan, A. De Tomaso, B. Davidson, A. Di Gregorio, M. Gelpke, D. M. Goodstein, et al. 2002. The draft genome of *Ciona intestinalis*: insights into chordate and vertebrate origins. *Science*. **298**: 2157–2167.
- Satou, Y., T. Kawashima, Y. Kohara, and N. Satoh. 2003. Large scale EST analyses in *Ciona intestinalis*: its application as Northern blot analyses. *Dev. Genes Evol.* **213**: 314–318.

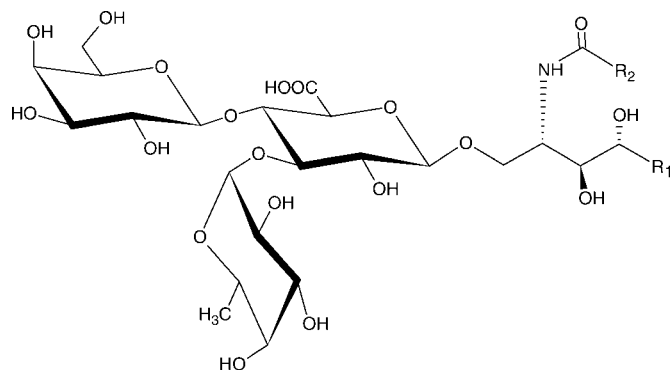


Fig. 6. Chemical structure of UGL-1. R1, sphingoid; R2, fatty acid. For the combination of R1 and R2, see Table 3.

14. Yamada, L., K. Kobayashi, Y. Satou, and H. Satoh. 2005. Microarray analysis of localization of maternal transcripts in eggs and early embryos of the ascidian, *Ciona intestinalis*. *Dev. Biol.* **284**: 536–550.
15. Ishibashi, T., T. Usami, M. Fujie, K. Azumi, N. Satoh, and S. Fujiwara. 2005. Oligonucleotide-based microarray analysis of retinoic acid target genes in the protochordate, *Ciona intestinalis*. *Dev. Dyn.* **233**: 1571–1578.
16. Aiello, A., E. Fattorusso, and M. Menna. 1996. Low molecular weight metabolites of three species of ascidians collected in the lagoon of Venice. *Biochem. Syst. Ecol.* **24**: 521–529.
17. Duran, R., M. J. Zubia, S. Nanjo, and J. Salva. 1998. Phallusides, new glucosphingolipids from the ascidian *Phallusia fumigata*. *Tetraedron.* **54**: 14597–14602.
18. Aiello, A., E. Fattorusso, A. Mangoni, and M. Menna. 2002. Sulciceramide, a novel triglycosylceramide from the marine ascidian *Microcosmus sulcatus*. *Eur. J. Org. Chem.* **6**: 1047–1050.
19. Hori, T., M. Sugita, S. Ando, K. Tsukada, K. Shiota, M. Tsuzuki, and O. Itasaka. 1983. Isolation and characterization of a 4-O-methyl-gucuronic acid-containing glycosphingolipid from spermatozoa of a fresh water bivalve, *Hyriopsis schlegelii*. *J. Biol. Chem.* **258**: 2239–2245.
20. Sugita, M., M. Nishida, and T. Hori. 1982. Studies on glycosphingolipids of larvae of the green-bottle fly, *Lucilia caesar*. I. Isolation and characterization of glycosphingolipids having novel sugar sequences. *J. Biochem. (Tokyo)*. **92**: 327–334.
21. Sugita, M., Y. Iwasaki, and T. Hori. 1982. Studies on glycosphingolipids of larvae of the green-bottle fly, *Lucilia caesar*. II. Isolation and structural studies of three glycosphingolipids with novel sugar sequences. *J. Biochem. (Tokyo)*. **92**: 881–887.
22. Itonori, S., M. Takahashi, T. Kitamura, K. Aoki, J. T. Dulaney, and M. Sugita. 2004. Microwave-mediated analysis for sugar, fatty acid, and sphingoid compositions of glycosphingolipids. *J. Lipid Res.* **45**: 574–581.
23. Kishimoto, Y., and M. Hoshi. 1972. Isolation, purification, and assay of fatty acids and steroids from the nervous system. In *Methods of Neurochemistry*. Vol. 3. R. Fried, editor. Marcel Dekker, New York. 75–154.
24. Ciucanu, I., and F. Kerek. 1984. A simple and rapid method for the permethylation of carbohydrates. *Carbohydr. Res.* **131**: 209–217.
25. Suzuki, Y., M. Suzuki, E. Ito, N. Goto-Inoue, K. Miseki, J. Iida, Y. Yamazaki, M. Yamada, and A. Suzuki. 2006. Convenient structural analysis of glycosphingolipids using MALDI-QIT-TOF mass spectrometry with increased laser power and cooling gas flow. *J. Biochem. (Tokyo)*. **139**: 771–777.
26. Seppo, A., M. Moreland, H. Schweingruber, and M. Tiemeyer. 2000. Zwitterionic and acidic glycosphingolipids of the *Drosophila melanogaster* embryo. *Eur. J. Biochem.* **267**: 3549–3558.
27. Hoshi, M., and Y. Nagai. 1975. Novel sialosphingolipids from spermatozoa of the sea urchin *Anthocidaris crassispina*. *Biochim. Biophys. Acta.* **388**: 152–162.
28. Kubo, H., A. Irie, F. Inagaki, and M. Hoshi. 1990. Gangliosides from the eggs of the sea urchin, *Anthocidaris crassispina*. *J. Biochem. (Tokyo)*. **108**: 185–192.
29. Shogomori, H., K. Chiba, and M. Hoshi. 1997. Association of the major gangliosides in sea urchin eggs with yolk lipoproteins. *Glycobiology*. **7**: 391–398.
30. Ijuin, T., K. Kitajima, Y. Song, S. Kitazume, S. Inoue, S. M. Jaslam, H. R. Morris, A. Dell, and Y. Inoue. 1996. Isolation and identification of novel sulfated and nonsulfated oligosialyl glycosphingolipids from sea urchin sperm. *Glycoconj. J.* **13**: 401–413.
31. Ohta, K., C. Sato, T. Matsuda, M. Toriyama, W. J. Lennarz, and K. Kitajima. 1999. Isolation and characterization of low density detergent-insoluble membrane (LD-DIM) fraction from sea urchin sperm. *Biochem. Biophys. Res. Commun.* **258**: 616–623.
32. Ilyas, A. A., M. C. Dalakas, R. O. Brady, and R. H. Quarles. 1986. Sulfated glycuronyl glycolipids reacting with anti-myelin-associated glycoprotein monoclonal antibodies including IgM paraproteins in neuropathy: species distribution and partial characterization of epitopes. *Brain Res.* **385**: 1–9.
33. Ogawa-Goto, K., Y. Ohta, K. Kubota, N. Funamoto, T. Abe, T. Taki, and K. Nagashima. 1993. Glycosphingolipids of human peripheral nervous system myelins isolated from cauda equina. *J. Neurochem.* **61**: 1398–1403.
34. Morikawa, K., K. Tsuneki, and K. Ito. 2001. Expression patterns of HNK-1 carbohydrate and serotonin in sea urchin, amphioxus, and lamprey, with reference to the possible evolutionary origin of the neural crest. *Zoology*. **104**: 81–90.
35. Nagai, Y. 1995. Functional roles of gangliosides in bio-signaling. *Behav. Brain Res.* **66**: 99–104.
36. Yu, R. K., H. Yoshino, M. Yamawaki, J. E. Yoshino, and T. Ariga. 1994. Subcellular distribution of sulfated glycuronyl glycolipids in human peripheral motor and sensory nerves. *J. Biomed. Sci.* **1**: 167–171.
37. Yamamoto, A., I. Yano, M. Masui, and E. Yabuuchi. 1978. Isolation of a novel sphingoglycolipid containing glucuronic acid and 2-hydroxy fatty acid from *Flavobacterium devorans* ATCC 10829. *J. Biochem. (Tokyo)*. **181**: 149–151 (Tokyo).
38. Kawahara, K., U. Seydel, M. Matsuura, H. Danbara, E. T. Rietschel, and U. Zahring. 1991. Chemical structure of glycosphingolipids isolated from *Sphingomonas paucimobilis*. *FEBS Lett.* **292**: 107–110.
39. Kawasaki, S., R. Moriguchi, K. Sekiya, T. Nagai, E. Ono, K. Kume, and K. Kawahara. 1994. The cell envelope structure of the lipopolysaccharide-lacking Gram-negative bacterium *Sphingomonas paucimobilis*. *J. Bacteriol.* **176**: 284–290.